IEEE Access
Multidisciplinary ⋮ Rapid Review ⋮ Open Access Journal

Received 27 November 2023, accepted 21 December 2023, date of publication 25 December 2023,
date of current version 8 January 2024.

Digital Object Identifier 10.1109/ACCESS.2023.3347222

RESEARCH ARTICLE

Low-Sidelobe Flat Panel Array Fed by a 3D-Printed Half-Mode Gap Waveguide Amplitude-Tapering Network

ADRIAN CASTELLÁ-MONTORO[1], (Student Member, IEEE), MIGUEL FERRANDO-ROCHER[2], (Senior Member, IEEE), JOSE IGNACIO HERRANZ-HERRUZO[2], (Member, IEEE), AND ALEJANDRO VALERO-NOGUEIRA[2], (Senior Member, IEEE)

[1]Institut National des Sciences Appliquées de Rennes, 35708 Rennes, France
[2]Departamento de Comunicaciones, Universitat Politècnica de València, 46022 Valencia, Spain

Corresponding author: Adrian Castellá-Montoro (Adrian.Castella-Montoro@insa-rennes.fr)

This work was supported in part by MCIN/AEI/10.13039/501100011033, and in part by "ERDF A Way of Making Europe" under Project PID2019-107688RB-C22 and Project PID2022-141055NB-C21.

ABSTRACT This article presents the design and evaluation of an 8 × 8 Ka-band low-sidelobe slot array antenna using gap waveguide technology. The slot array is fed by a single-layer amplitude-tapering network implemented in half-mode groove gap waveguide, resulting in a low-profile, low-sidelobe antenna. The simplicity of the proposed feeding network, composed of a novel design of asymmetrical dividers, enables precise fabrication using cost-effective additive techniques. Experimental results demonstrate a significant reduction in sidelobe levels compared to traditional uniform arrays, with a radiation efficiency exceeding 84%. This design, featuring simple and robust asymmetrical splitters, is well-suited for applications requiring high gain and low interference.

INDEX TERMS Antenna arrays, bed of nails, gap waveguide, half-mode waveguide, Ka-band, low side lobe, Taylor distribution, SATCOM.

I. INTRODUCTION

In the last few years, the fifth-generation (5G) wireless communications system has attracted a great deal of interest and has developed rapidly. To meet the growing demand for fast and reliable network access, the 5G system must have high capacity and low latency. So, the demand for high-data-rate communication systems has surged in the millimeter-wave band [1], [2].

Conventionally, reflector antennas are used to provide the directional communication link. However, reflector antennas are expensive and difficult to manufacture due to their bulky structures. On the other hand, flat antennas, showing low profile and lightweight, become one the most attractive candidates to replace reflectors, though there are still challenges. Among them is the need for high antenna gain and efficiency. Conventional printed solutions, such as microstrip planar arrays, are flexible in design and manufacture, but with unacceptable ohmic loss in large millimeter-wave arrays [3], [4], [5]. On the other hand, flat-panel arrays fed by low-loss metallic waveguides become more suitable for their use in millimeter-wave applications [6], [7].

As it is well known, the first sidelobe level (SLL) of uniformly fed arrays is approximately -13.2 dB, which is not low enough for some applications. In this context, low-sidelobe antenna arrays have gained importance in high-performance wireless communication systems, such as satellite communications, to mitigate interference. An approach to achieving low SLL performance is to use uniformly excited tilted slots in a square array [8], [9]. However, an additional thick layer capable of rotating the orientation of the radiating slots relative to the main array planes must be added [10].

The associate editor coordinating the review of this manuscript and approving it for publication was Sandra Costanzo.

A continuous transverse stub system described in [11] achieves high gain and wide bandwidth, but only the H-plane SLL is suppressed. Note that most of the targeted applications require low SLL levels along all azimuthal angles.

Amplitude-tapering techniques are often employed to create low SLL antenna arrays by adjusting the power applied to each element through an appropriate feed network [12], [13], [14], being Taylor's distribution a well-established and versatile method. Due to the high gain requirement, a certain amount of radiating elements, excited by a large feeding network, is needed, often leading to bulky waveguide structures. Hence, achieving compact waveguide feed networks with suitable power weighting is challenging, and in many cases, they are difficult to manufacture [15], [16], [17], [18]. In [15], a double-layer corporate-fed slot array antenna is proposed. The feeding network layer synthesizes a Taylor distribution, being the unit cell a cavity-backed 2 × 2 slots subarray. Within a given unit cell, the four slots are fed with the same amplitude and phase, leading to a quasi-Taylor array distribution. This fact entails a perceptible SLL increase at around 30°-50° elevation angle.

In the context of metal-based waveguides, over the past decade, there has been significant progress in the study of Gap Waveguide (GW) structures [19], with Groove Gap Waveguide (GGW) [20] and Ridge Gap Waveguide (RGW) [21] being extensively examined. Typically, in GGWs, the groove forming the waveguide is integrated into the Bed Of Nails (BoN) in a single piece. Consequently, any bends, curves, or transitions along the groove affect the adjacent nails, causing them to become narrower and thinner. A recently proposed alternative approach, as detailed in [22] and [23], is known as Half-Mode Groove Gap Waveguide (HM-GGW), and it entails manufacturing the waveguide and BoN as separate components. The significant advantage lies in the ease of manufacturing, as the groove does not interfere with the standard pin layout. Additionally, the BoN component can be standardized and reused for other devices. This technology appears better suited to design low SLL antennas with fewer layers, enabling an easier fabrication of the amplitude-tapering feeding networks, and becoming more convenient for mass production.

This paper applies Taylor synthesis to design a non-uniform power distribution waveguide network in HM-GGW technology. Novel unequal waveguide splitters are proposed to build the intricate feeding network, resulting in a compact single-layer structure, robust against manufacturing tolerances. These unequal power dividers can achieve large power ratios between output ports with small phase differences of less than 5°. As a result, the full network feeds an 8 × 8 slot array to obtain a suitable power distribution among the antenna elements, achieving a low SLL high-efficiency array. Unlike previous developments, an individual array weighting is successfully achieved. The final antenna array takes advantage of the benefits of HM-GGW technology, i.e., its low profile, high efficiency, and robustness against fabrication tolerances [23]. This fact is demonstrated by fabricating a prototype with additive techniques, showing a good electrical performance. The remainder of the paper is organized as follows. Section II describes the feeding network with the novel implementation of unequal power splitters in HM-GGW technology. In Section III, the integration of the feeding network to create a slotted antenna array is presented. The antenna manufacture and the experimental results are reported in Section IV. Finally, Section V draws the main conclusions of this work.

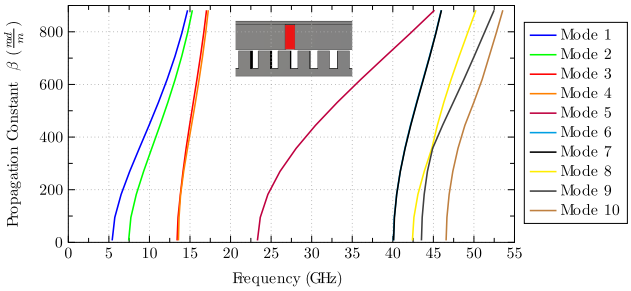

FIGURE 1. Dispersion diagram of the HM-GGW.

TABLE 1. Design parameters of the HM-GGW structure.

Variables	Geometrical sizes (mm)
Air gap	0.2
Length of nails	2.6
Width of nails	0.8
Nail periodicity	1.8
Height of HM-GGW	3.88
Width of HM-GGW	1

II. FEEDING NETWORK DESIGN

A. HM-GGW BANDGAP

The electromagnetic bandgap (EBG) of the HM-GGW is first illustrated in Fig. 1. It can be observed that the BoN creates a stopband between 15 GHz and 40 GHz, and within the band of interest of our design (29 GHz - 31 GHz), only the fundamental mode (Mode 5), equivalent to a half-TE_{10}, propagates along the HM-GGW. An air gap of $\lambda_0/20$, where λ_0 is the free-space wavelength at the center frequency, is left between the BoN and the feeding network. The length of the nails is $\lambda_0/4$, approximately, to function as an AMC (*Artificial Magnetic Conductor*). The height of the HM-GGW is half the length of a horizontally-polarized GGW (3.88 mm in this case) [24]. The nail height-to-width ratio is typically 2:1, and the nail periodicity is $0.2\lambda_0$ [25]. Table 1 shows the design parameters of the HM-GGW structure.

B. UNEQUAL POWER SPLITTERS

The low-sidelobe characteristic of the antenna array relies on a proper amplitude-tapering feed network enabled by a robust and versatile design of unequal power dividers. Specifically, this work proposes novel unequal T-junction splitters in HM-GGW technology. Such waveguide realiza-

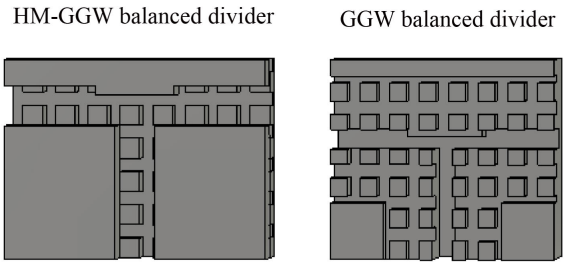

FIGURE 2. Schematic of a balanced HM-GGW (left) and GGW (right) power divider.

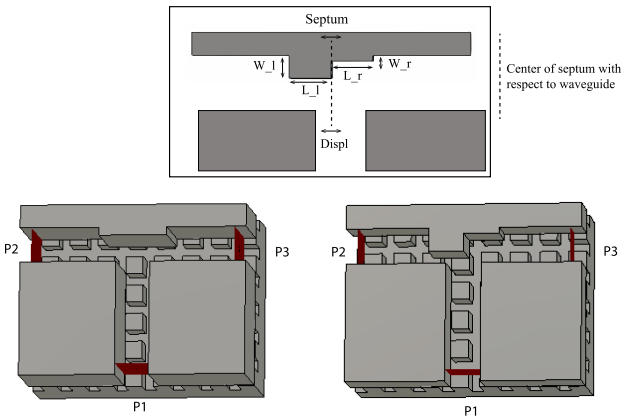

FIGURE 3. Schematic of a balanced (left) and unbalanced (right) power T-junction splitter in HM-GGW technology.

tion has demonstrated [23] appealing design and fabrication advantages over conventional GGWs. In fact, Fig. 2 compares a balanced T-Junction divider in HM-GGW technology and its equivalent in GGW technology. It can be appreciated that in HM-GGW technology, the waveguide and the BoN are built in separate layers so nails remain intact. In contrast to splitters in GGW technology, nails do not need to be thinned to accommodate the waveguide, thus improving the robustness and the manufacturing ease. In addition, it is noteworthy to stress that the HM-GGW version reduces the coupling between nearby waveguides [23], which becomes essential when designing large arrays.

The T-junction splitters shown in Fig. 2 provide an equal power distribution because of the structure symmetry. Furthermore, the phase difference produced between the output ports is 180°, as a horizontally-polarized HM-GGW is employed. In order to achieve a wideband impedance matching, a centered septum [26] has been used.

This simple divider architecture can be easily modified to achieve an unbalanced T-junction splitter. The idea is to use septums of different widths to achieve the desired power unbalance.

The overall structure of the proposed balanced and unbalanced dividers in HM-GGW technology can be seen in Fig. 3. In addition to the asymmetric width, the septum center can be slightly shifted with respect to the input waveguide to improve phase difference and the power ratio response. The splitter structure is defined by the variables shown in Fig. 3. Therefore, splitters with a power imbalance of up to

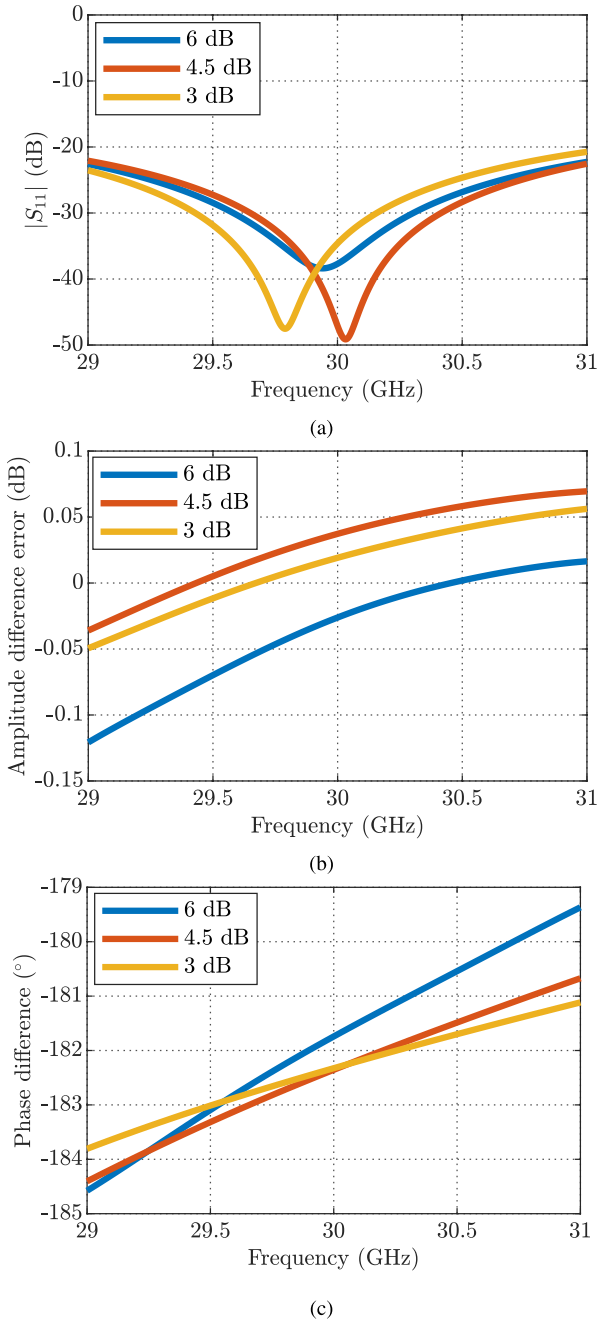

FIGURE 4. S-parameters of 6 dB,4.5 dB and 3 dB unequal splitters: (a) S_{11}; (b) power ratio error between output ports; (c) Phase difference between output ports.

6 dB or even more can be achieved by controlling only these five septum parameters. Fig. 4 show the performance of 2:1 splitters with an unbalance of 3, 4.5 and 6 dB respectively, achieving good matching (below −20 dB), power and phase imbalance less than 0.12 dB and 5 degrees between the output ports respectively, in the band of interest. Table 2 shows the dimensions of HM-GGW unequal power dividers.

It is worth mentioning at this point that it is not trivial at all to design unbalanced waveguide dividers with high output power ratios and small phase differences, in addition to a

TABLE 2. Dimensions of the unequal power dividers.

Power Ratio	3 dB	4.5 dB	6 dB
W_l (mm)	0.72	0.83	0.88
L_l (mm)	2.82	2.74	2.84
W_r (mm)	0.39	0.36	0.25
L_r (mm)	2.83	2.75	2.85
Disp (mm)	0.03	0.035	0.03
Input/output width (mm)	1	1	1

TABLE 3. Comparison with other unbalanced splitters.

Ref.	P.R (dB)	P.R.E (dB)	P.D.E (°)
[15]	5.58	0.30	15
[16]	2.67	1	*
[27]	6	0.5	12
[28]	6	2	4
[18]	5.61	0.3	9
Our work	**6**	**0.12**	**5**

P.R: Power Ratio; PRE: Power Ratio Error; P.D.E: Phase Difference Error
*unknown P.D.E

wide input impedance bandwidth. Such specifications often lead to critical dimensions which compromise the robustness and reliability of the fabrication process. In this sense, the novel HM-GGW splitter architecture adopted in this work enables low-cost 3D manufacturing technologies rarely found in low-sidelobe waveguide arrays.

Table 3 presents a comparison of different unequal power splitters from the existing literature. Splitters used in [15] exhibit a phase difference of more than 15 degrees between the output ports. Furthermore, in [16] and [27], splitters with a limited power ratio are developed, resulting in worse SLL levels. Finally, in [28] dividers with high return loss and small phase imbalance between output ports are designed. However, the desired power ratio over the whole bandwidth is not properly maintained. In contrast, in this work splitters of 6 dB power ratio with less than 0.12 dB power ratio error and 5 degrees of phase imbalance are achieved. For large arrays, minimizing these phase difference and power ratio errors is crucial as they are cumulative along the whole network, leading to undesired results.

C. TAYLOR DISTRIBUTION DESIGN

An 8 × 8 element power distribution network has been built with the power dividers presented. A 25-dB Taylor distribution has been adopted along both planes, resulting in three different horizontal and vertical power distribution levels. In Fig. 5, the first splitters present a balanced power ratio at the center of the distribution network in both planes. The next horizontal and vertical splitters need power ratios of 6 dB, 1.48 dB, and 5.77 dB, sorted from the input to the output ports.

With these computed amplitude ratios, the optimal unequal HM-GGW splitters, constituting the 8 × 8 distribution network, have been fine-tuned. Consequently, the designed

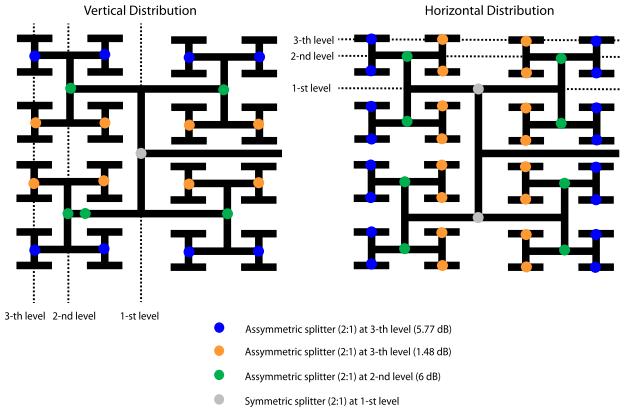

FIGURE 5. Schematic of the power distribution ratios for the 8 × 8-element feeding network.

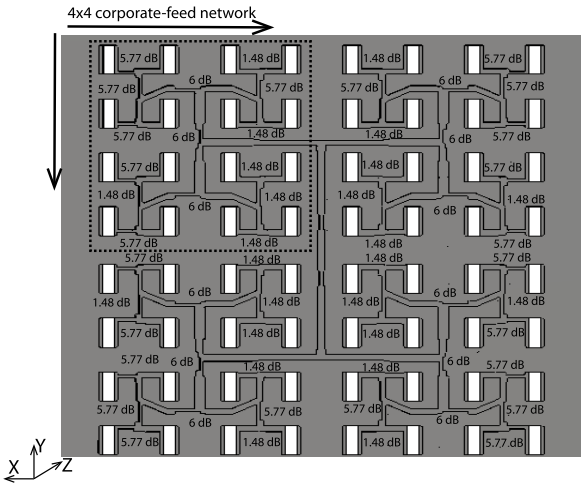

FIGURE 6. Corporate-feed network in HM-GGW for 8 × 8 elements.

feeding network can be divided into four quadrants, with 4×4 outputs each. These quadrants are identical but mirrored, directing the majority of power toward the central outputs, as illustrated in Fig. 6.

III. ANTENNA DESIGN

The architecture of the designed antenna array is shown in Fig. 7. It comprises only two pieces. The first one consists of the equispaced BoN and the input port (WR-28), whereas the second layer comprises the Taylor feed network (bottom face) and the slot elements (upper face). The radiating element consists of a rectangular slot fed by a short-circuited HM-GGW. In order to maximize the field coupling, the slot is located $\lambda/4$ away from the waveguide shortcircuit.

The array spacing is $0.8\lambda_0 \times 0.9\lambda_0$ along the x- and y-axis, respectively, to minimize the appearance of grating lobes as much as possible. Radiating slot dimensions are optimized to maximize the element bandwidth. The bandwidth is mostly dominated by the main dimensions of the radiating slot (l_s and w_s).

In this regard, narrow enough radiating elements have been chosen to avoid unwanted cross-polarization effects [29].

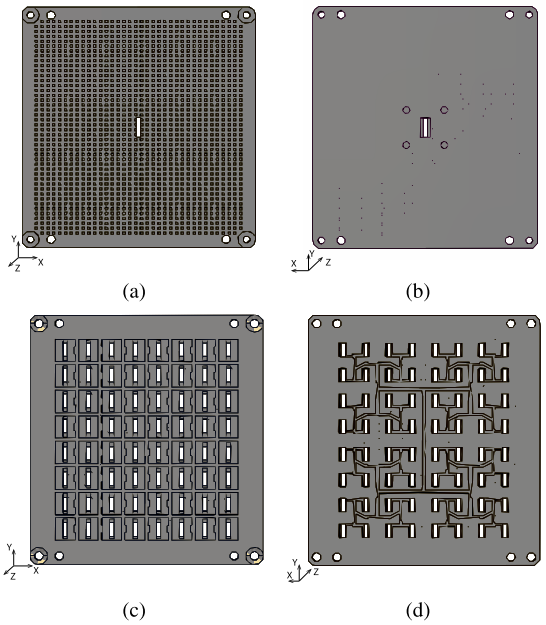

FIGURE 7. Layers of the 8 × 8 antenna: first layer a) and b), second layer c) and d). a) BoN (top view), b) input port (rear view), c) radiating slots (top view), d) feeding network (rear view).

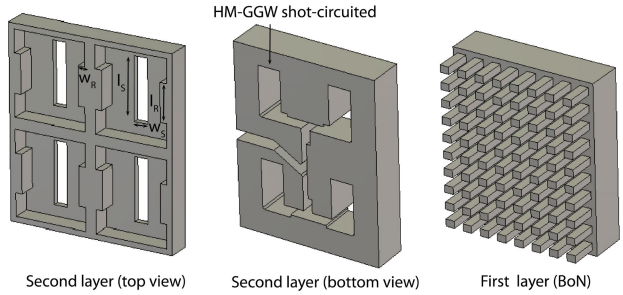

FIGURE 8. Configuration of the 2 × 2 unit cell.

In order to enhance the limited impedance bandwidth of rectangular slots [30], they have been surrounded by a double-ridged open cavity [23], [31]. Finally, a compact realization of a typical chandelier-type feeding is adopted to compensate for the 180-degree shift of the HM-GGW T-splitters, as shown in Fig. 8.

IV. EXPERIMENTAL RESULTS

The antenna assembly was fabricated using the Selective Laser Melting (SLM) 3D printing technique. The total dimensions of the prototype are 88 mm × 80 mm in surface and 14.9 mm in height. An image of the manufactured antenna with both layers can be seen in Fig. 9. Fig. 10 plots the measured S_{11}-parameter at the input port compared to simulation. Return loss better than 10 dB has been measured from 29.7 GHz to 31.87 GHz.

Fig. 11 displays the measured directivity, simulated gain, and measured gain versus frequency. The entire measured band achieves an overall radiation efficiency above 84% (29.5 to 31.87 GHz). The measurements have been performed in the anechoic chamber of our own laboratory. A slight

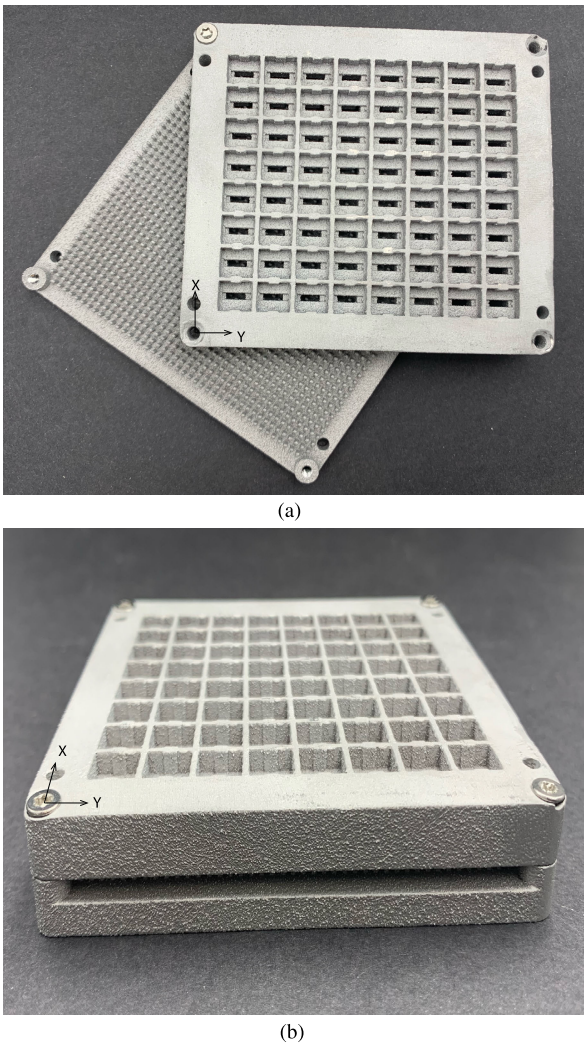

FIGURE 9. Photographs of the manufactured antenna using selective laser melting (SLM). (a) Top view. (b) Lateral view.

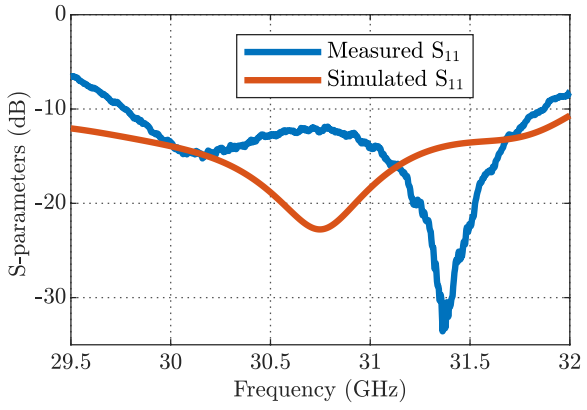

FIGURE 10. Simulated and measured S_{11}-parameter.

deviation of 0.5 dB between simulated and measured gain is observed, which is to be expected, even more so due to the 3D printing technique tolerances and the surface roughness. The ideal, simulated, and measured radiation patterns at 30 GHz are presented in Fig. 12. The measured XZ- and YZ-plane sidelobe levels are better than −22 dB, and cross-polarization

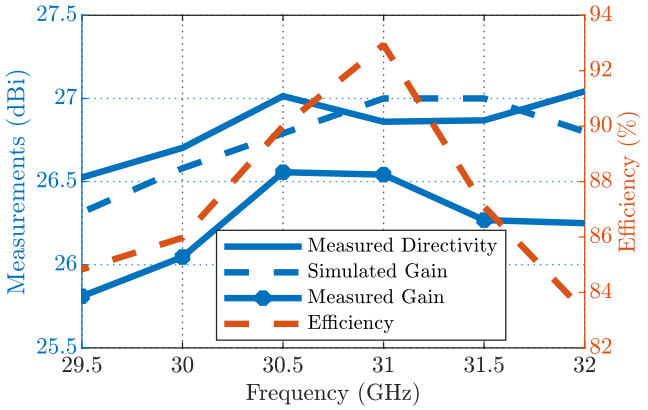

FIGURE 11. Measured directivity, simulated and measured gain, and radiation efficiency versus frequency.

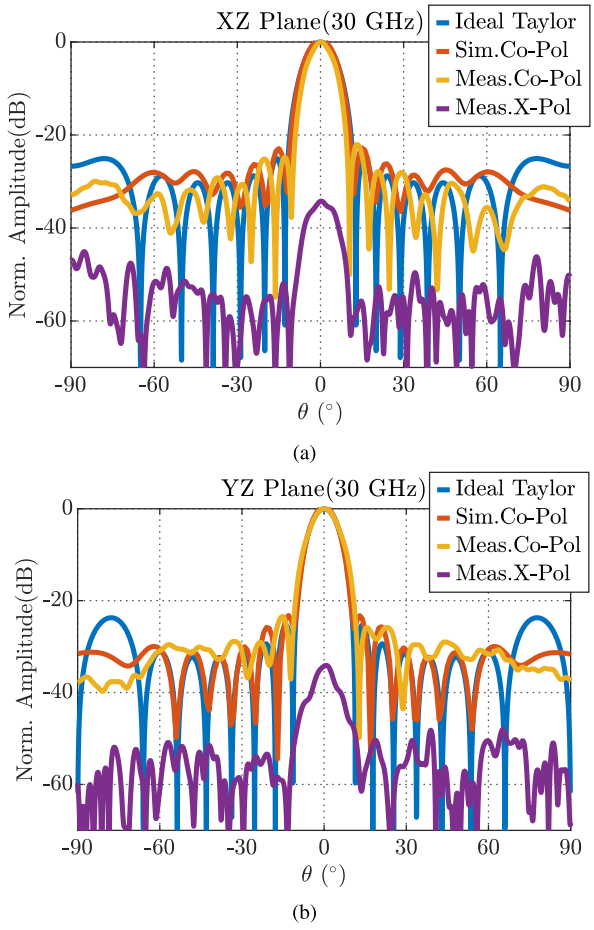

FIGURE 12. Simulated and measured radiation patterns at 30 GHz: (a) XZ- and (b) YZ-plane.

discriminations (XPD) above 30 dB are recorded at the center frequency. Finally, the measured radiation patterns at the edge frequencies (29 and 31 GHz) are shown in Fig. 13.

Table 4 presents a comparison of the antenna characteristics with several low-SLL antennas from the existing literature. Our proposed approach significantly enhances the radiation efficiency compared to previous studies while maintaining minimal sidelobes within a straightforward, compact, and purely metallic structure, ideal for SATCOM

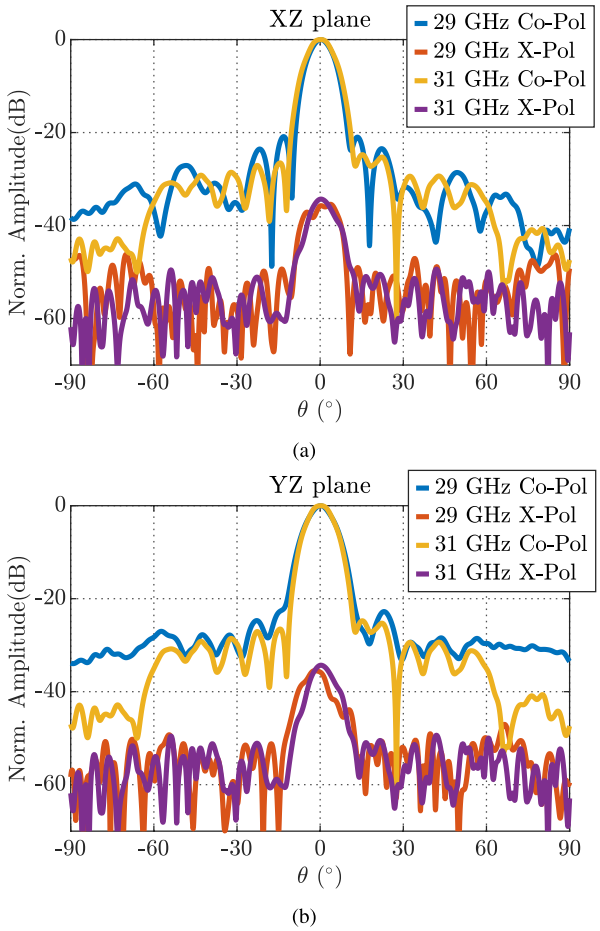

FIGURE 13. Measured radiation patterns at 29 GHz and 31 GHz in (a) XZ- and (b) YZ- plane.

applications. Furthermore, our antenna design lends itself well to fabrication using current additive manufacturing techniques, thereby reducing associated production costs, being a highly considered alternative given the current rise of 3D printing structures in the field of wireless communications [36]. It is worth noting that in [15] and [28], an additional layer known as the backed cavity is introduced to enhance coupling. As a result, it deviates from the strict definition of Taylor distribution (referred to as quasi-Taylor), as each output of the feeding network excites a group of four slots uniformly. In contrast, in our work, the feed network is able to individually excite each radiating slot with the required weight, improving the array synthesis and approaching the ideal SLL performance. Furthermore, [32] and [33] make use of an additional layer, besides the feeding network and the radiating element layers, to avoid mutual coupling so that the SLL response is not compromised. In our design, such a layer is not necessary since the HM-GGW technology naturally reduces the coupling level thanks to the intact BoN homogeneity. Finally, in [18], two different layers are used to perform the Taylor amplitude tapering, which results in a more complex and bulky structure, less appropriate for mass production.

TABLE 4. Performance comparison of low-sidelobe antennas.

Ref.	Full Metal structure	IB	Freq.Band	RE	SideLobe Level	Fabrication Cost	Number of Layers	Dimensions
[15]	Yes	13.8	Ku	70	-24.1	High	4	12.18×12.18×0.9
[16]	No	16	Ka	42	-18	Low	4	8.15×8.15×1.4
[17]	Yes	6	E	79	-20.5	Med.	1	15.61×1.40×3
[18]	Yes	19.2	E	70	-21	Med-High	3	8.40×8.40×1.84
[27]	No	33	Ka	30	-14	Med.	3	6.50×6.50×1
[28]	No	18.5	V	50	-23	Med.	4	13.18×13.18×*
[32]	Yes	13.6	Ka	70	-18	Med.	3	11.10×8.50×1.07
[33]	Yes	0.34	X	30	-28.8	Med.	3	7.27×7.27×*
[34]	Yes	6.8	E	70	-20	High.	7	17.75×17.75×*
Our work	**Yes**	**7.2**	**Ka**	**84**	**-22**	**Low-Med.**	**2**	**8.80×8.00×1.2**

IB: Impedance Bandwidth (-10 dB) (%); RE: Realized Radiation Efficiency (%) [35]; Dimensions: Dimensions in terms of central wavelength; * unknown dimension

V. CONCLUSION

This paper introduces an 8 × 8 Ka-band antenna array, composed of a novel and simple design of asymmetrical dividers, harnessing the Half-Mode Groove Gap waveguide technology. This recent waveguide version is better suited for practical industrial manufacturing when compared to other technologies such as GGW. The developed antenna boasts a single-layer amplitude-tapering feeding network and maintains a compact, purely metallic structure using just two metal pieces. The experimental findings showcase its effective reduction in sidelobe levels, high radiation efficiency, and stable performance across a broad bandwidth. The use of additive manufacturing techniques further underscores the viability of our approach for scalable mass production, being a very suitable option for SATCOM applications.

REFERENCES

[1] E. Feltrin and E. Weller, "New frontiers for the mobile satellite interactive services," in *Proc. 5th Adv. Satell. Multimedia Syst. Conf. 11th Signal Process. Space Commun. Workshop*, Sep. 2010, pp. 155–161.

[2] M. M. Abdin, W. Joel, D. Johnson, and T. M. Weller, "A system and technology perspective on future 5G mm-wave communication systems," in *Proc. IEEE 18th Wireless Microw. Technol. Conf. (WAMICON)*, Apr. 2017, pp. 1–6.

[3] H. A. Diawuo, S. J. Lee, and Y.-B. Jung, "Sidelobe-level reduction of a linear array using two amplitude tapering," *IET Microw. Antenna Propag.*, vol. 11, no. 10, pp. 1432–1437, Aug. 2017.

[4] H. Wang, D.-G. Fang, and X. G. Chen, "A compact single layer monopulse microstrip antenna array," *IEEE Trans. Antennas Propag.*, vol. 54, no. 2, pp. 503–509, Feb. 2006.

[5] W. Yang, K. Ma, K. S. Yeo, and W. M. Lim, "A compact high-performance patch antenna array for 60-GHz applications," *IEEE Antennas Wireless Propag. Lett.*, vol. 15, pp. 313–316, 2016.

[6] A. Vosoogh and P.-S. Kildal, "Corporate-fed planar 60-GHz slot array made of three unconnected metal layers using AMC pin surface for the gap waveguide," *IEEE Antennas Wireless Propag. Lett.*, vol. 15, pp. 1935–1938, 2016.

[7] A. Dorlé, R. Gillard, E. Menargues, M. Van Der Vorst, E. De Rijk, P. Martín-Iglesias, and M. García-Vigueras, "Circularly polarized leaky-wave antenna based on a dual-mode hollow waveguide," *IEEE Trans. Antennas Propag.*, vol. 69, no. 9, pp. 6010–6015, Sep. 2021.

[8] Y. You, Y. Lu, T. Skaik, Y. Wang, and J. Huang, "Millimeter-wave 45° linearly polarized corporate-fed slot array antenna with low profile and reduced complexity," *IEEE Trans. Antennas Propag.*, vol. 69, no. 9, pp. 6064–6069, Sep. 2021.

[9] T. Tomura, Y. Miura, M. Zhang, J. Hirokawa, and M. Ando, "A 45° linearly polarized hollow-waveguide corporate-feed slot array antenna in the 60-GHz band," *IEEE Trans. Antennas Propag.*, vol. 60, no. 8, pp. 3640–3646, Aug. 2012.

[10] Y. Miura, J. Hirokawa, M. Ando, Y. Shibuya, and G. Yoshida, "Double-layer full-corporate-feed hollow-waveguide slot array antenna in the 60-GHz band," *IEEE Trans. Antennas Propag.*, vol. 59, no. 8, pp. 2844–2851, Aug. 2011.

[11] T. Potelon, M. Ettorre, L. Le Coq, T. Bateman, J. Francey, D. Lelaidier, E. Seguenot, F. Devillers, and R. Sauleau, "A low-profile broadband 32-slot continuous transverse stub array for backhaul applications in *E*-band," *IEEE Trans. Antennas Propag.*, vol. 65, no. 12, pp. 6307–6316, Dec. 2017.

[12] R. C. Hansen, "Contributions of T.T. Taylor to array synthesis," in *Proc. IEEE Antennas Propag. Soc. Int. Symp.*, Jul. 1998, pp. 2294–2297.

[13] M. Zatman, "Low sidelobe taper choice for wideband adaptive arrays," in *Proc. IEEE Antennas Propag. Soc. Int. Symp.*, vol. 1, Jun. 1998, pp. 192–194.

[14] G. D. Hopkins, J. Ratner, A. Traille, and V. Tripp, "Aperture efficiency of amplitude weighting distributions for array antennas," in *Proc. IEEE Aerosp. Conf.*, Mar. 2007, pp. 1–9.

[15] G.-L. Huang, S.-G. Zhou, T.-H. Chio, H.-T. Hui, and T.-S. Yeo, "A low profile and low sidelobe wideband slot antenna array feb by an amplitude-tapering waveguide feed-network," *IEEE Trans. Antennas Propag.*, vol. 63, no. 1, pp. 419–423, Jan. 2015.

[16] X. Jiang, F. Jia, Y. Cao, P. Huang, J. Yu, X. Wang, and Y. Shi, "Ka-band 8 × 8 low-sidelobe slot antenna array using a 1-to-64 high-efficiency network designed by new printed RGW technology," *IEEE Antennas Wireless Propag. Lett.*, vol. 18, no. 6, pp. 1248–1252, Jun. 2019.

[17] K. Lomakin, S. Alhasson, and G. Gold, "Additively manufactured amplitude tapered slotted waveguide array antenna with horn aperture for 77 GHz," *IEEE Access*, vol. 10, pp. 44271–44277, 2022.

[18] P. Liu, G. F. Pedersen, and S. Zhang, "Wideband low-sidelobe slot array antenna with compact tapering feeding network for E-band wireless communications," *IEEE Trans. Antennas Propag.*, vol. 70, no. 4, pp. 2676–2685, Apr. 2022.

[19] A. Valero-Nogueira, E. Alfonso, J. I. Herranz, and P.-S. Kildal, "Experimental demonstration of local quasi-TEM gap modes in single-hard-wall waveguides," *IEEE Microw. Wireless Compon. Lett.*, vol. 19, no. 9, pp. 536–538, Sep. 2009.

[20] A. Jiménez Sáez, A. Valero-Nogueira, J. I. Herranz, and B. Bernardo, "Single-layer cavity-backed slot array fed by groove gap waveguide," *IEEE Antennas Wireless Propag. Lett.*, vol. 15, pp. 1402–1405, 2016.

[21] E. Alfonso, M. Baquero, P.-S. Kildal, A. Valero-Nogueira, E. Rajo-Iglesias, and J. I. Herranz, "Design of microwave circuits in ridge-gap waveguide technology," in *IEEE MTT-S Int. Microw. Symp. Dig.*, May 2010, pp. 1544–1547.

[22] M. Ferrando-Rocher, J. I. Herranz-Herruzo, A. Valero-Nogueira, and M. Baquero-Escudero, "Half-mode waveguide based on gap waveguide technology for rapid prototyping," *IEEE Microw. Wireless Compon. Lett.*, vol. 32, no. 2, pp. 117–120, Feb. 2022.

[23] M. Ferrando-Rocher, J. I. Herranz-Herruzo, A. Valero-Nogueira, and M. Baquero-Escudero, "A half-mode groove gap waveguide for single-layer antennas in the millimeter-wave band," *IEEE Antennas Wireless Propag. Lett.*, vol. 21, no. 12, pp. 2402–2406, Dec. 2022.

[24] M. Ferrando-Rocher, A. Valero-Nogueira, and J. I. Herranz-Herruzo, "Exploring half-mode groove gap waveguide performance and advantages," in *Proc. 16th Eur. Conf. Antennas Propag. (EuCAP)*, Mar. 2022, pp. 1–4.

[25] M. F. Rocher. (2019). *Gap Waveguide Array Antennas and Corporate-Feed Networks for mm-Wave band Applications*. [Online]. Available: https://riunet.upv.es/handle/10251/115933
[26] M. Ferrando-Rocher, A. Valero-Nogueira, and J. I. Herranz-Herruzo, "New feeding network topologies for high-gain single-layer slot array antennas using gap waveguide concept," in *Proc. 11th Eur. Conf. Antennas Propag. (EUCAP)*, Mar. 2017, pp. 1654–1657.
[27] T. Li and Z. N. Chen, "Wideband sidelobe-level reduced *Ka*-band metasurface antenna array fed by substrate-integrated gap waveguide using characteristic mode analysis," *IEEE Trans. Antennas Propag.*, vol. 68, no. 3, pp. 1356–1365, Mar. 2020.
[28] J. Liu, F. Yang, K. Fan, and C. Jin, "Unequal power divider based on inverted microstrip gap waveguide and its application for low sidelobe slot array antenna at 39 GHz," *IEEE Trans. Antennas Propag.*, vol. 69, no. 12, pp. 8415–8425, Dec. 2021.
[29] K. Kelleher, W. Scott, and N. Marchand, "Cross polarization effects on antenna radiation patterns," in *Proc. IRE Int. Conv. Rec.*, Mar. 2005, pp. 153–159.
[30] F. Manshadi, "Small crossed-slot radiating elements for phased array applications," in *Proc. Antennas Propag. Soc. Symp. Dig.*, Jun. 1991, vol. 3, no. 1, pp. 1828–1831.
[31] T. Zhang, R. Tang, L. Chen, S. Yang, X. Liu, and J. Yang, "Ultra-wideband full-metal planar array antenna with a combination of ridge gap waveguide and E-plane groove gap waveguide," *IEEE Trans. Antennas Propag.*, vol. 70, no. 9, pp. 8051–8058, Sep. 2022.
[32] L. Shi, C. Bencivenni, R. Maaskant, J. Wettergren, J. Pragt, and M. Ivashina, "High-efficiency and wideband aperiodic array of uniformly excited slotted waveguide antennas designed through compressive sensing," *IEEE Trans. Antennas Propag.*, vol. 67, no. 5, pp. 2992–2999, May 2019.
[33] P. Kumar, A. Kedar, and A. K. Singh, "Design and development of low-cost low sidelobe level slotted waveguide antenna array in X-band," *IEEE Trans. Antennas Propag.*, vol. 63, no. 11, pp. 4723–4731, Nov. 2015.
[34] H. Arakawa, T. Tomura, and J. Hirokawa, "Sidelobe suppression in both the e and h planes using slit layers over a corporate-feed waveguide slot array antenna consisting of 2 × 2-element radiating units," *IEICE Trans. Commun.*, vol. E103.B, no. 9, pp. 960–968, 2020.
[35] *IEEE Standard Definitions of Terms for Radio Wave Propagation—IEEE Antennas and Propagation Society—IEEE Standard Definitions of Terms for Radio Wave Propagation*, IEEE Standard 145-2013, 2013.
[36] M. Garcia-Vigueras, L. Polo-Lopez, C. Stoumpos, A. Dorle, C. Molero, and R. Gillard, "Metal 3D-printing of waveguide components and antennas: Guidelines and new perspectives," *Hybrid Planar—3D Waveguiding Technologies*. London, U.K.: IntechOpen, Sep. 2022.

ADRIAN CASTELLÁ-MONTORO (Student Member, IEEE) was born in Murcia, Spain, in 1997. He received the B.E. and M.S. degrees in telecommunication engineering from Universitat Politècnica de València (UPV), Valencia, in 2020 and 2022, respectively. He is currently pursuing the Ph.D. degree with Institut National des Sciences Appliquées de Rennes (INSA), Rennes, France, with a focus on broadband 3D-printed phased arrays. In 2021, he joined the Antennas and Propagation Laboratory, Institute of Telecommunications and Multimedia Applications, UPV.

MIGUEL FERRANDO-ROCHER (Senior Member, IEEE) was born in Alcoy, Spain. He received the M.Sc. and Ph.D. degrees in telecommunication engineering from Universitat Politècnica de València (UPV), Valencia, Spain, in 2012 and 2018, respectively. In 2012, he joined the Complex Radiation Systems Team, Institut d'Electronique et des Technologies du numéRique (IETR), Rennes, France, as a Researcher, where he was involved in reflectarray antennas for satellite applications in collaboration with Thales Alenia Space France (TASF) and Thales Alenia Space Italy (TASI). Since 2013, he has been with the Antennas and Propagation Laboratory (APL), UPV. In 2016, he joined the Chalmers University of Technology, Gothenburg, Sweden, as a Guest Researcher. Since September 2019, he has been an Assistant Professor with the Department of Physics, Systems Engineering, and Signal Theory, University of Alicante, Alicante, Spain. Since 2023, he has been an Associate Professor with the Department of Communications, UPV. He also collaborates with the Microwave and Applied Computational Electromagnetics Group (GMECA) in Alicante for his research activities. His current research interests include satellite communication (SATCOM) on-the-move, high-gain antennas and arrays, gap waveguide (GW) technology, and millimeter-wave components. He was a recipient of the Extraordinary Prize for Doctoral Theses from UPV, in 2020, the AIRBUS Defense and Space Award, in 2019, and the URSI Conference Best Student Paper Award, in 2017. Since 2022, he has been an Ambassador of the IEEE Young Professionals Program to inspire and inform future generations on a variety of technical and non-technical topics in the field of antennas and propagation.

JOSE IGNACIO HERRANZ-HERRUZO (Member, IEEE) was born in Valencia, Spain, in 1978. He received the M.S. and Ph.D. degrees in telecommunication engineering from Universitat Politècnica de València (UPV), Valencia, in 2002 and 2015, respectively. In 2002, he joined the Antennas and Propagation Laboratory, Institute of Telecommunications and Multimedia Applications, UPV. In 2005, he became an Assistant Professor and he has been an Associate Professor with the Communications Department, UPV, since 2019. His current research interests include the numerical modeling and design of waveguide slot arrays and the application of gap waveguide technology to the design of microwave and millimeter-wave antennas and components.

ALEJANDRO VALERO-NOGUEIRA (Senior Member, IEEE) was born in Madrid, Spain, in 1965. He received the degree in telecommunication engineering from Universidad Politècnica de Madrid, Madrid, in 1991, and the Ph.D. degree in telecommunication from Universitat Politècnica de València, Valencia, Spain, in 1997. In 1992, he joined Departamento de Comunicaciones, Universitat Politècnica de València, where he is currently a Full Professor. In 1999, he was on leave at the ElectroScience Laboratory, The Ohio State University, Columbus, OH, USA, where he was involved in fast solution methods in electromagnetics (EMs) and conformal antenna arrays. His current research interests include computational EMs, waveguide slot arrays, gap waveguides (GW), and the theory of characteristic modes.